Hyo Yun Jung, Mihai Stoica, Seong Hoon Yi, Do Hyang Kim, Jürgen Eckert

Influence of Al on glass forming ability and nanocrystallization behavior of cast-iron based bulk amorphous alloy

Erstveröffentlichung in / First published in:

Journal of Materials Research. 2015, 30(6), S. 818-824 [Zugriff am: 13.03.2020]. Cambridge University Press. ISSN 2044-5326.

DOI: https://doi.org/10.1557/jmr.2015.48

Influence of Al on glass forming ability and nanocrystallization behavior of cast-iron based bulk amorphous alloy

Hyo Yun Jung[a)]
Institute for Complex Materials, IFW Dresden, D-01069 Dresden, Germany

Mihai Stoica
Institute for Complex Materials, IFW Dresden, D-01069 Dresden, Germany; and Politehnica University of Timisoara, 300006 Timisoara, Romania

Seong Hoon Yi
Department of Materials Science and Metallurgical Engineering, Kyungpook National University, Daegu 702-701, South Korea

Do Hyang Kim
Department of Metallurgical Engineering, Center for Non-crystalline Materials, Yonsei University, 120-749 Seoul, South Korea

Jürgen Eckert[b)]
Institute for Complex Materials, IFW Dresden, D-01069 Dresden, Germany; and Institute of Materials Science, University of Technology Dresden, D-01062 Dresden, Germany

(Received 16 October 2014; accepted 17 February 2015)

Cast-iron (CI) based bulk amorphous alloy with compositions of $Fe_{75.5-x}C_{6.0}Si_{3.3}B_{5.5}P_{8.7}Cu_{1.0}Al_x$ (x = 0, 1 at.%) was synthesized by Cu mold casting. As indicated by increased critical diameters (d_{max}) for the amorphization, the substitution of Al enhanced the glass-forming ability of the alloy. However, the onset temperature of crystallization (T_x) and the range of supercooled liquid region (ΔT_x) of the alloy decreased upon Al addition from 500 °C and 28 °C to 475 °C and 25 °C, respectively. It was revealed that the decreased thermal stability of the amorphous phase is related to the enhanced crystallization tendency to form primary α-Fe phase. Upon the nanocrystallization of primary α-Fe phase the Al-added alloy shows enlarged M_s of 176 emu g^{-1}, still keeping a reasonable small H_c value of 0.086 Oe. The present study revealed that the minor Al addition enhances not only the glass-forming ability, but also the nanocrystallization behavior of the CI based bulk amorphous alloy.

I. INTRODUCTION

Soft magnetic nanocrystalline alloys prepared with Fe-based amorphous precursor are well known to have high saturation magnetization (M_s), low saturation magnetostriction (λ_s), and high initial permeability (μ_i).[1,2] The excellent soft magnetic properties of the alloys are attributed to the special microstructure consisted of fine ferromagnetic phases with typical size of ~25 nm and residual amorphous matrix.[3–5] Randomly dispersed nano-scaled ferromagnetic phases can reduce the effective magnetocrystalline anisotropy of the amorphous alloy, consequently resulting ultrasoft magnetic characteristics.[6]

Recently, developments of soft magnetic nanocrystalline alloys with amorphous precursor having high M_s, and low material cost have attracted great attention owing to increasing industrial demand for functional soft magnetic materials. In the past few years, lots of Fe-based amorphous alloys and bulk metallic glasses (BMGs) have been widely studied to synthesize Fe-nanocrystalline alloys.[7–14] Optimizing the composition and microstructure, the alloys having high M_s and excellent magnetic softness have been newly developed in various Fe–metalloid–Cu alloy systems: $Fe_{85.2}Si_1B_9P_4Cu_{0.8}$,[11] $(Fe_{0.5}Co_{0.5})_{73.5}Si_{13.5}B_9Nb_3Cu_1$,[12] $Fe_{83}P_{13}Si_3Cu_1$,[13] and $(Fe_{0.8}P_{0.09}C_{0.09}B_{0.2})_{99.3}Cu_{0.7}$.[14] However, for extensive industrial application of the materials, good combination of low material cost, high productivity, and excellent functional properties is required. In previous studies, Yi and Jung[15] reported successful development of Fe-based BMGs with cheap raw materials of commercial cast-iron (CI) and industrial ferro-alloys. Because the alloys have high glass-forming ability (GFA) as well as good mechanical, electrical, and soft magnetic properties,

Contributing Editor: Michael E. McHenry
[a)]Address all correspondence to this author.
e-mail: hyoyun.jung@gmail.com
[b)]This author was an editor of this focus issue during the review and decision stage. For the *JMR* policy on review and publication of manuscripts authored by editors, please refer to http://www.mrs.org/jmr-editor-manuscripts/.
DOI: 10.1557/jmr.2015.48

they have been considered to have high industrial potential. Recently, it was further revealed that the soft magnetic properties of the CI based BMGs with an alloy composition of $Fe_{76.0}C_{6.0}Si_{3.3}B_{5.5}P_{8.7}Cu_{0.5}$ (at.%) can be further enhanced by optimum nanocrystallization of α-Fe phase.[16] Thus, the investigation on the synthesis of the nanocrystalline alloy based on these CI based BMG is drawing further attention.

Crystallization products as well as crystallization kinetics of the soft magnetic Fe-based nanocrystalline alloys are strongly related to composition.[5] Thus, there have been many studies about the effect of a minor element addition/substitution on the crystallization behavior and soft magnetic properties.[17–24] Among them, there are reports showing that small Al addition can be also beneficial to enhance the soft magnetic properties of Fe-based nanocrystalline alloys.[21–24] As for example, in the case of FINEMET-type alloy, it was reported that the 1.0 at.% Al addition enhances the μ_i at 1 kHz. Lim et al.[21] insisted that the minor Al addition reduces the grain size of α-FeSi phase and decreases the intrinsic magnetocrystalline anisotropy K_1. On the other hand, Chen et al.[24] reported that minor addition of Al or Si enhances the μ of Fe–Zr–B alloys by changing their λ_s from a negative value to near zero. In addition, because the metalloids such as B, C, Si, Al, and Ga have negative heat when mixing with Fe, the addition of these elements enhances the GFA of the amorphous alloys.[25] On the other hand, Al or Ga does not form their own compounds in amorphous matrix, but is only properly soluble in α-Fe or other metalloid-compounds.[26] Thus, the minor Al addition in Fe-based amorphous alloys can be expected to be beneficial for GFA as well as to promote the soft magnetic nanocrystallization.

Because there has been no investigation on the minor Al addition on the nanocrystallization behavior of the CI-based BMGs, the present study aims to investigate the effect of the 1 at.% Al addition on GFA, soft magnetic properties, and nanocrystallization behavior of the $Fe_{75.5}C_{6.0}Si_{3.3}B_{5.5}P_{8.7}Cu_{1.0}$ (at.%) CI based BMG.

II. MATERIAL AND METHODS

Master alloys with nominal compositions of $Fe_{75.5-x}C_{6.0}Si_{3.3}B_{5.5}P_{8.7}Cu_{1.0}Al_x$ (x = 0, 1 at.%) were prepared under a Ti-gettered argon atmosphere by arc melting of CI; industrial Fe–P alloy; and pure elements of Fe (99.7% purity), Si (99.99% purity), B (99.5% purity), Al (99% purity), and Cu (99.98%, purity). The composition of industrial raw materials (CI and Fe–P) is listed in Table I. Ribbons with about 35 μm thickness and 2 mm wide were prepared by single roll melt spinning. Cylindrical specimens having a length of 55 mm and a diameter of 1, 2, and 3 mm were prepared by suction casting. The structure of the as-prepared and annealed specimens was characterized using x-ray diffraction (XRD, Panalytical X'pert Pro, Almelo, Netherlands) with Co radiation (λ = 0.179 nm). Thermal analysis was performed by differential scanning calorimetry (DSC, PYRIS Diamond, Perkin Elmer Instruments, Norwalk, CT) and differential thermal analysis (DTA, S-1600, Sinco, Seoul, South Korea). The as-cast specimens were annealed in DSC to achieve partial crystallization of amorphous phase. Magnetic properties were determined using an alternating gradient magnetometer under maximum applied magnetic field of 2 kOe.

III. RESULTS AND DISCUSSION

The structural analysis of the as-cast $Fe_{75.5}C_{6.0}Si_{3.3}B_{5.5}P_{8.7}Cu_{1.0}$ and $Fe_{74.5}C_{6.0}Si_{3.3}B_{5.5}P_{8.7}Cu_{1.0}Al_{1.0}$ (at.%) rods with a diameter of 1, 2, and 3 mm was performed by XRD patterns presented in Fig. 1. In the case of Al-free alloy, the suction cast rod having a diameter of 1 mm shows a broad halo pattern characteristic for an amorphous phase, while the rod with 2 mm diameter exhibits sharp diffraction peaks of Fe_3C, Fe_2P, α-Fe, and $Fe_{23}C_6$ phases. On the other hand, the alloy containing 1 at.% Al shows the formation of an amorphous rod with a diameter of 2 mm. Thus, the critical diameter (d_{max}) of the Al-free alloy and Al-added alloy for amorphization is 1 and 2 mm, respectively.

Figure 2 shows DTA melting curves of the as-cast $Fe_{75.5}C_{6.0}Si_{3.3}B_{5.5}P_{8.7}Cu_{1.0}$ and

TABLE I. Chemical composition of CI and ferro-phosphorus alloy.

	(wt%)							
	Fe	C	Si	P	S	Ni	Ti	Cu
CI	95.060	4.280	0.460	0.200	0.034	0.094	0.029	...
Fe–P	73.161	0.015	0.009	26.83	0.012	...	0.350	0.004

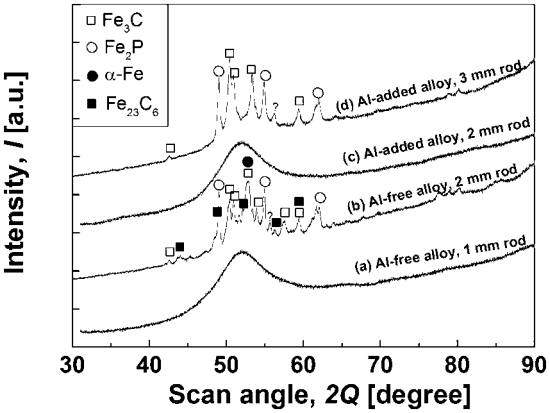

FIG. 1. XRD patterns of the as-cast $Fe_{75.5}C_{6.0}Si_{3.3}B_{5.5}P_{8.7}Cu_{1.0}$ and $Fe_{74.5}C_{6.0}Si_{3.3}B_{5.5}P_{8.7}Cu_{1.0}A_{l1.0}$ (at.%) rods with different diameters (1, 2, and 3 mm).

$Fe_{74.5}C_{6.0}Si_{3.3}B_{5.5}P_{8.7}Cu_{1.0}Al_{1.0}$ amorphous rods with 1 mm diameter. It is observed that the substitution of Al for 1 at.% Fe has insignificant influence on the melting behavior. Both alloys have highly overlapped endothermic peaks, indicating that the composition of the alloys is located near eutectic point. On the other hand, the Al addition slightly decreases the liquidus temperature (T_l) of the alloy from 1016 to 1008 °C. The instrumental error of temperature in these measurements is typically ±0.5 to 1.0 °C. It is well known that the amorphous alloy having the composition near eutectic composition and low T_l tend to have high GFA.[27] With a consideration of increased d_{max} of the alloy, one can conclude that the 1 at.% Al addition enhances GFA of the Fe–C–Si–B–P–Cu BMG by stabilizing the undercooled liquid.[28]

Figure 3 shows DSC heating curves of the as-cast $Fe_{75.5}C_{6.0}Si_{3.3}B_{5.5}P_{8.7}Cu_{1.0}$ and $Fe_{74.5}C_{6.0}Si_{3.3}B_{5.5}P_{8.7}Cu_{1.0}Al_{1.0}$ (at.%) rods having a diameter of 1 mm. For comparison, the DSC curves of the as-spun ribbon are also shown in Fig. 3. The as-spun ribbon and rod of both alloys have no appreciable difference in DSC curve, which might be attributed to similar crystallization behavior of the specimens. During continuous heating of amorphous rod with a heating rate of 40 °C/min, both alloys show clear Curie temperature (T_C) of about 360 ± 0.5 °C and distinct glass transition followed by a wide supercooled liquid region. These results indicate that the alloys formed amorphous phase having high thermal stability and strong ferromagnetic characteristics. On the other hand, it is observed that the 1 at.% Al addition decreases glass transition temperature (T_g) and onset crystallization temperature (T_x) of the alloy from 472 ± 1.0 °C and 500 ± 0.5 °C to 450 ± 1.0 °C and 476 ± 0.5 °C, respectively. It is notable that T_g and T_x of the Al-added alloy are dramatically reduced by 1 at.% Al addition, suggesting that Al addition decreases the barrier to crystallization from the as-cast state.

To investigate the crystallization product(s) of each crystallization stage of the alloys shown in Fig. 3, the specimens were heated up to the peak temperature of crystallization curve (T_p = 2 °C). Figure 4 shows XRD patterns of the partially crystallized

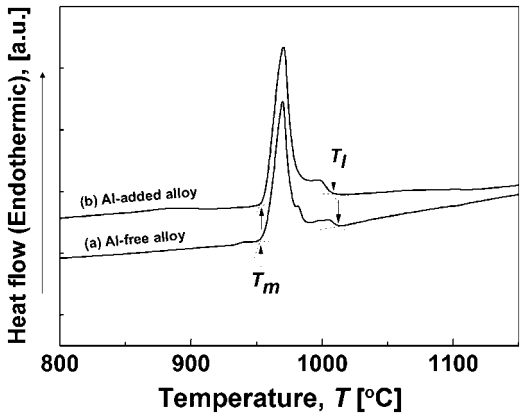

FIG. 2. Melting curves of the as-cast $Fe_{75.5}C_{6.0}Si_{3.3}B_{5.5}P_{8.7}Cu_{1.0}$ and $Fe_{74.5}C_{6.0}Si_{3.3}B_{5.5}P_{8.7}Cu_{1.0}Al_{1.0}$ rods having a diameter of 1 mm.

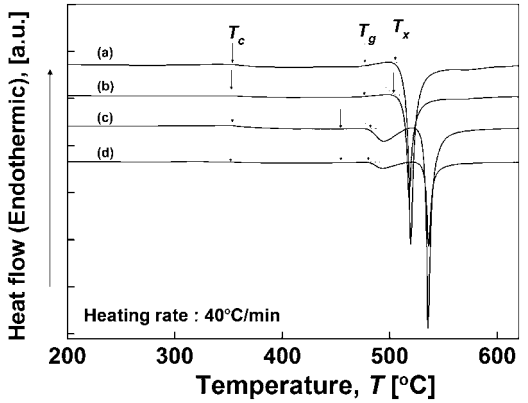

FIG. 3. Continuous DSC heating curves of (a) as-cast $Fe_{75.5}C_{6.0}Si_{3.3}B_{5.5}P_{8.7}Cu_{1.0}$ rod (Φ = 1 mm), (b) as-spun $Fe_{75.5}C_{6.0}Si_{3.3}B_{5.5}P_{8.7}Cu_{1.0}$ ribbon, (c) as-cast $Fe_{74.5}C_{6.0}Si_{3.3}B_{5.5}P_{8.7}Cu_{1.0}Al_{1.0}$ rod (Φ = 1 mm), and (d) as-spun $Fe_{74.5}C_{6.0}Si_{3.3}B_{5.5}P_{8.7}Cu_{1.0}Al_{1.0}$ ribbon.

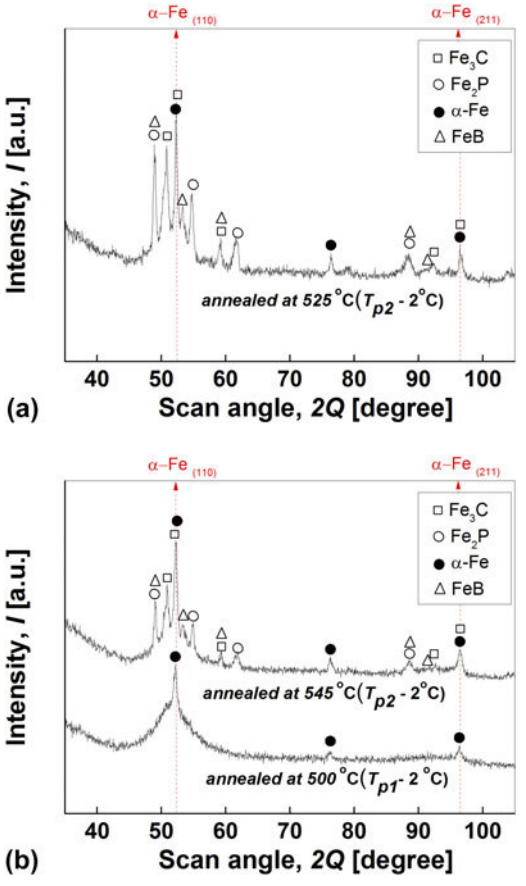

FIG. 4. XRD patterns of the (a) $Fe_{75.5}C_{6.0}Si_{3.3}B_{5.5}P_{8.7}Cu_{1.0}$ and (b) $Fe_{74.5}C_{6.0}Si_{3.3}B_{5.5}P_{8.7}Cu_{1.0}Al_{1.0}$ rods annealed at primary or secondary crystallization stage.

$Fe_{75.5}C_{6.0}Si_{3.3}B_{5.5}P_{8.7}Cu_{1.0}$ and $Fe_{74.5}C_{6.0}Si_{3.3}B_{5.5}P_{8.7}Cu_{1.0}Al_{1.0}$ (at.%) rods having a diameter of 1 mm. The Al-free alloy having single crystallization stage shows the XRD pattern consisted of a mixture of Fe_3C, α-Fe, Fe_2P, and FeB phases. This indicates that the Al-free alloy has almost simultaneous crystallization of various stable and metastable phases. On the other hand, it is observed that the primary crystallization peak of the Al-containing alloy is related to the formation of α-Fe phase. After that the Al-added alloy also forms various Fe–metalloid compounds, i.e., Fe_3C, Fe_2P, and FeB phases in its secondary crystallization step. Therefore, it is clear that the 1 at.% Al addition changes the crystallization behavior of the alloy from eutectic-type crystallization to primary-type crystallization. Also, it is revealed that the decreased thermal stability of supercooled liquid of Al-added alloy is directly related to the enhanced crystallization tendency of primary α-Fe phase.

To minimize demagnetizing effect and magnetic anisotropy caused by geometrical characteristics of the specimens,[29] the influence of the 1 at.% Al addition on soft magnetic properties of the amorphous alloys was examined upon hysteresis *M-H* loops of the as-spun ribbon (Fig. 5). Both alloys exhibit narrow *M-H* hysteresis loop, indicating good magnetic softness of the alloys. The 1 at.% Al addition leads to minor reduction of M_s from 144 ± 3 emu g^{-1} to 142 ± 3 emu g^{-1}, and enlargement of H_c from 0.11 to 0.13 Oe. As a function of annealing temperature (T_a), the variation in M_s and H_c of the alloys was further investigated with short-term isothermal annealing for 60 s with a heating rate of 40 °C/min (Fig. 6). It is notable that both alloys annealed up to T_a of 450 °C have decreased H_c with almost constant M_s. However, the Al-added alloy starts to show an increase of M_s with T_a of 470 °C. The alloy has a decrease of M_s with T_a of 540 °C. On the other hand, the Al-free alloy shows an enhancement of M_s only with T_a of 490 and 500 °C. After that the Al-free alloy has a significant decrease of M_s and increase of H_c with annealing at T_a of 520 °C. Figure 7 shows XRD patterns of the ribbons annealed at the temperature of 460, 480, 500, and 520 °C. It is revealed that the enhancement of M_s of the alloys is attributed to the formation of α-Fe as a primary phase. The Al-free alloy annealed at 520 °C has sequential formation of various Fe–metalloid compounds of Fe_3C, Fe_2P, and FeB phases, which causes the deterioration of magnetic softness of the alloy. Figure 8 compares the hysteresis *M-H* loops of the Al-free and Al-added alloys annealed at 520 °C. While the Al-added alloy has narrow hysteresis *M-H* loop with low H_c of 86 mOe and high M_s of 176 emu g^{-1}, it is notable that the Al-free alloy annealed at 520 °C shows significant deterioration of magnetic softness, showing high H_c of 18 Oe and decreased M_s of 138 emu g^{-1}. Considering that the Al-added alloy also shows deterioration of magnetic softness at annealing temperature of 540 °C, we can conclude that the temperature range for nanocrystallization of α-Fe phase of Al-free alloy is from 500 °C to below 510 °C, and that of Al containing alloy is from 470 to 530 °C. Referring to Fig. 3, the valid temperature range for nanocrystallization of the Al-free alloys is

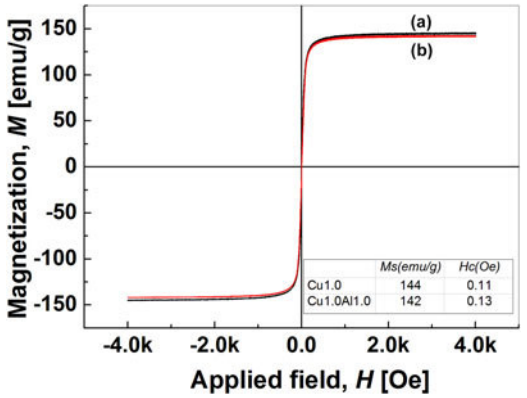

FIG. 5. *M-H* hysteresis loop of as-spun (a) $Fe_{75.5}C_{6.0}Si_{3.3}B_{5.5}P_{8.7}Cu_{1.0}$ and (b) $Fe_{74.5}C_{6.0}Si_{3.3}B_{5.5}P_{8.7}Cu_{1.0}Al_{1.0}$ ribbon.

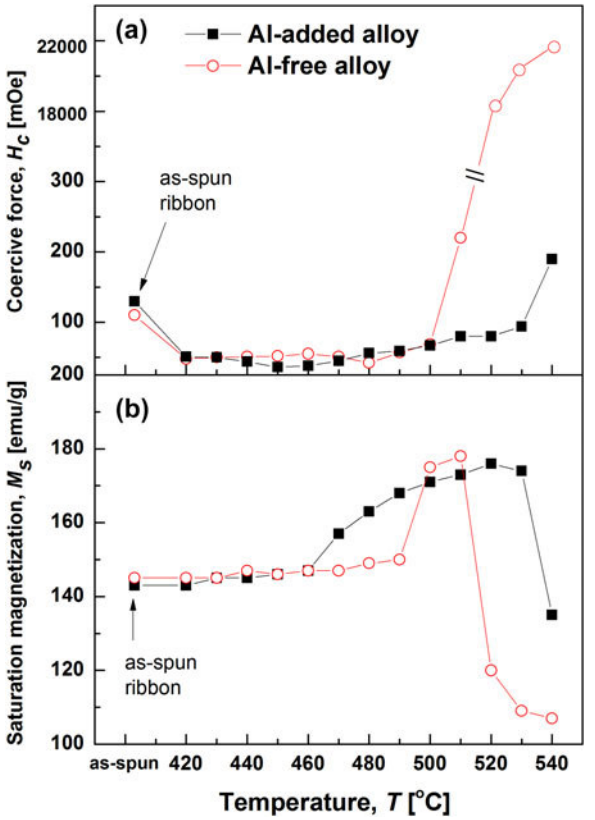

FIG. 6. Variation of (a) saturation magnetization (M_s) and (b) coercive force (H_c) of $Fe_{75.5}C_{6.0}Si_{3.3}B_{5.5}P_{8.7}Cu_{1.0}$ and $Fe_{74.5}C_{6.0}Si_{3.3}B_{5.5}P_{8.7}Cu_{1.0}Al_{1.0}$ ribbon as a function of annealing temperature.

located only in the narrow temperature range of supercooled liquid region, while the Al-added alloy can have it from the temperature around T_g to the offset temperature of primary crystallization peak. Thus, it is clear that the minor Al addition significantly influences the thermal stability of the precursor and residual amorphous matrix of the alloys. While the minor alloying of 1 at.% Al has insignificant influence on the general soft magnetic properties of the alloy in the as-spun state, it changes the thermal stability of the amorphous structure, and thus the soft magnetic properties of nanocrystallized specimen were strongly influenced by Al addition.

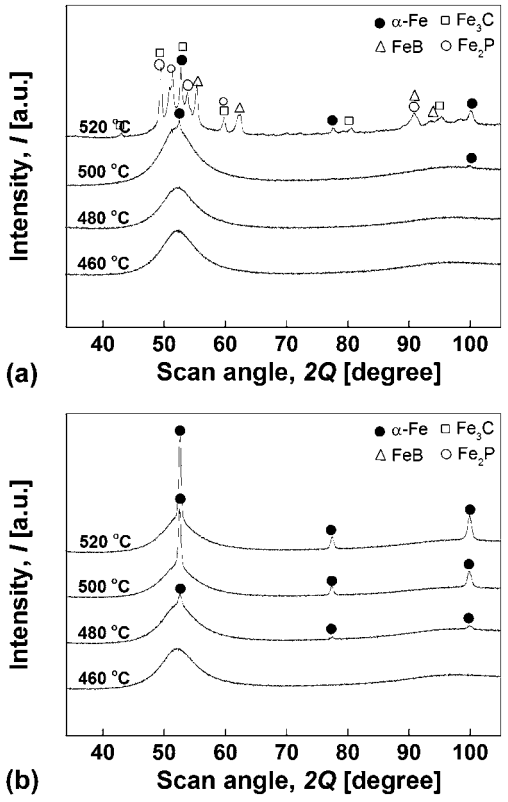

FIG. 7. XRD patterns of the (a) $Fe_{75.5}C_{6.0}Si_{3.3}B_{5.5}P_{8.7}Cu_{1.0}$ and (b) $Fe_{74.5}C_{6.0}Si_{3.3}B_{5.5}P_{8.7}Cu_{1.0}Al_{1.0}$ ribbon as a function of annealing temperature.

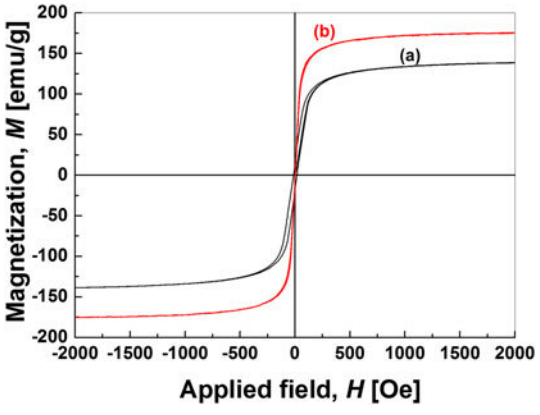

FIG. 8. *M-H* hysteresis loop of (a) $Fe_{75.5}C_{6.0}Si_{3.3}B_{5.5}P_{8.7}Cu_{1.0}$ and (b) $Fe_{74.5}C_{6.0}Si_{3.3}B_{5.5}P_{8.7}Cu_{1.0}Al_{1.0}$ ribbon annealed for 60 s at 520 °C.

The above results demonstrate that the Al-added alloy has wider temperature range for the formation of nanoscaled α-Fe phase. The minor Al addition enhances the crystallization tendency of α-Fe phase in amorphous phase, but rather suppresses further crystallization of the residual amorphous phase. That is, the Al-addition promotes the primary crystallization of α-Fe phase, and stabilizes the residual amorphous matrix.

It is well known that the thermal stability of supercooled liquid is primarily related to the initial crystallization rate of the primary phase. According to Ohnuma et al.,[30] the kinetics of Cu-clustering in amorphous phase is strongly related to the Cu contents. Due to the same Cu contents of the present Al-free and Al-added alloys, one can expect that the Al addition does not significantly influence the kinetics of Cu-clustering in amorphous phase. Thus, it is reasonable that the initial crystallization rate of α-Fe phase can be affected by the heterogeneous nucleation rate. In Fig. 4, we investigated the crystallization behavior of the Al-free alloy and Al-added alloy. Table II lists the interplanar spacing $d_{(hkl)}$ of (110) and (211) planes of the α-Fe phase formed in Al-free and Al-containing alloys. Considering details of α-Fe phase of the alloys, one can note that the lattice parameter of α-Fe phase ($a_{\alpha\text{-Fe}}$) of Al-added alloy is continuously changing as crystallization proceeds. The $d_{(110)}$ of α-Fe phase during primary crystallization stage and secondary crystallization stage is 2.036 ± 0.001 Å and 2.031 ± 0.001 Å, respectively. Thus, the α-Fe phase initially formed during primary crystallization of the Al-added alloy has larger $a_{\alpha\text{-Fe}}$ than α-Fe phase in the later crystallization stage of the alloy. Ohkubo et al.[18] investigated heterogeneous nucleation of α-Fe phase on Cu clusters. They revealed that the special orientational matching between (110) plane of α-Fe phase and (111) plane of Cu clusters having fcc structure reduces interface energy, resulting enlarged nucleation rate of primary α-Fe phase. In the case of present Al-added alloy, it can be known that the (110) plane of α-Fe phase of the alloy containing Al has better matching with (111) plane of free-Cu clusters ($d_{(111)}$ = 2.087 Å).[31] Thus, it is expectable that the high

TABLE II. Interplanar spacing of the (110) and (211) planes of α-Fe phase formed in Al-free and Al-containing alloys.

	Annealing temperature (°C)	$d_{(110)}$ (Å)	$d_{(211)}$ (Å)
Al-free alloy	T_{p1} = 2	2.031	1.200
Al-added alloy	T_{p1} = 2	2.036	1.201
	T_{p2} = 2	2.031	1.200

solubility of Al during the initial crystallization of α-Fe phase promoted heterogeneous nucleation rate, and thus the thermal stability of amorphous phase was decreased due to the enhanced crystallization tendency to form α-Fe phase.

Alternatively, regarding the enhanced thermal stability of residual amorphous phase of the Al-added alloy after primary crystallization, it was shown that the Al atoms are diffused out to the residual amorphous matrix. In the case of Al-added Nanoperm-alloy,[24] it was also revealed that the Al atoms are preferably placed at the boundary of primary phase. As shown in Fig. 4, Al in the present alloy does not form any compounds during secondary crystallization of residual amorphous phase. Thus, in the present alloy, the existence of Al around α-Fe grains may delay the atomic rearrangement and thus the crystallization of residual amorphous phase can be suppressed.

In the previous study,[32] the present authors investigated the optimum Cu contents for the nanocrystallization of α-Fe phase in Fe–C–Si–B–P–Cu BMGs. Analyzing the crystallization behavior of the $Fe_{76.5-x}C_{6.0}Si_{3.3}B_{5.5}P_{8.7}Cu_x$ (x = 0, 0.5, and 1.0 at.%) alloy, we concluded that the Cu 1.0 at.% addition is not an optimum Cu content for the nanocrystallization of single α-Fe phase in Fe–C–Si–B–P–Cu BMGs, because it provides excess heterogeneous nucleation site not only to primary α-Fe phase, but also to the other Fe–metalloid compounds. However, in the present study, it has been revealed that the alloy with Cu 1.0 at.% can modify the initial crystallization behavior through the minor 1.0 at.% Al addition. As the Al addition promotes the crystallization of primary α-Fe phase but stabilizes the residual amorphous matrix, the alloy could have further enhanced nanocrystallization behavior of the α-Fe phase. Moreover, it was also seen that the Al addition improves the GFA of the alloy. Thus, one can conclude that the Al addition is beneficial to make the alloy good amorphous precursor of soft magnetic nanocrystalline BMGs.

IV. CONCLUSIONS

We have studied the GFA, soft magnetic properties, and nanocrystallization behavior of the $Fe_{75.5}C_{6.0}Si_{3.3}B_{5.5}P_{8.7}Cu_{1.0}$ and $Fe_{74.5}C_{6.0}Si_{3.3}B_{5.5}P_{8.7}Cu_{1.0}Al_{1.0}$ (at.%) alloys. Substitution for Fe by 1 at.% Al enhanced GFA as well as changed crystallization behavior of the alloy. It was found that the minor Al addition can improve the GFA of the alloy with increase of d_{max} for glass formation. The reduced T_x and ΔT_x of the Al-added alloy demonstrates the decreased thermal stability of the amorphous phase with enhanced crystallization tendency to form α-Fe phase. While the Al-free alloy has almost simultaneous formation of various phases, but the minor Al addition leads to primary crystallization of α-Fe phase with temperature of about 80 °C. In spite of minor effect of Al addition on the M_s, H_c, and T_C of the amorphous alloy, the 1 at.% Al addition enhanced magnetic softness as well as M_s of the alloy with formation of nanosized α-Fe phase. Because the present Fe–C–Si–B–P–Cu–Al BMG has high GFA and good soft magnetic properties with high M_s of 176 emu g^{-1}, the alloy can be one of the good candidates as an amorphous precursor of soft magnetic nanocrystalline BMGs having high industrial potential.

ACKNOWLEDGMENTS

This work was supported by the Global Research Laboratory Program of the Korea Ministry of Science and Technology. The support of the German Science Foundation (DFG) through the grants STO 873/2-1 and STO 873/2-2 is also acknowledged.

REFERENCES

1. H.R. Lashgari, D. Chua, S. Xie, H. Sun, M. Ferry, and S. Li: Composition dependence of the microstructure and soft magnetic properties of Fe-based amorphous/nanocrystalline alloys: A review study. *J. Non-Cryst. Solids* **391**, 61 (2014).
2. A.M. Leary, P.R. Ohodnicki, and M.E. McHenry: Soft magnetic materials in high-frequency, high-power conversion applications. *JOM* **64**, 772 (2012).
3. Y. Yoshizawa, S. Oguma, and K. Yamauchi: New Fe-based soft magnetic alloys composed of ultrafine grain structure. *J. Appl. Phys.* **64**, 6044 (1988).
4. K. Suzuki, A. Makino, N. Kataoka, A. Inoue, and T. Masumoto: High saturation magnetization and soft magnetic properties of bcc Fe-Zr-B and Fe-Zr-B-M (M = transition metal) alloys with nanoscale grain size. *Mater. Trans., JIM* **32**, 93 (1991).
5. T. Kulik: Nanocrystallization of metallic glasses. *J. Non-Cryst. Solids* **287**, 145 (2001).
6. G. Herzer: Grain size dependence of coercivity and permeability in nanocrystalline ferromagnets. *IEEE Trans. Magn.* **26**, 1397 (1990).
7. M. Ohta and Y. Yoshizawa: New high-B_s Fe-based nanocrystalline soft magnetic alloys. *Jpn. J. Appl. Phys.* **46**, L477 (2007).
8. A. Makino, H. Men, T. Kubota, K. Yubuta, and A. Inoue: FeSiBPCu nanocrystalline soft magnetic alloys with high Bs of 1.9 tesla produced by crystallizing hetero-amorphous phase. *Mater. Trans.* **50**, 204 (2009).
9. A. Inoue and X.M. Wang: Bulk amorphous FC20 (Fe–C–Si) alloys with small amounts B and their crystallized structure and mechanical properties. *Acta Mater.* **48**, 1383 (2000).
10. S.N. Kane, H.J. Lee, Y.H. Jeong, and L.K. Varga: Cast iron (CI) based soft magnetic BMG $Ci_{88.3}Al_2Ga_1P_{4.35}B_{4.35}$. *J. Phys.: Conf. Ser.* **144**, 012040 (2009).
11. K. Takenaka, M. Nishijima, and A. Makino: Effect of metalloid elements on the structures and soft magnetic properties in $Fe_{85.2}Si_xB_{14-x-y}P_yCu_{0.8}$ alloys. *IEEE Trans. Magn.* **50**(4), 2004704 (2014).
12. T. Gheiratmand, H.R. Madaah Hosseini, P. Davami, M. Gjoka, G. Loizos, and H. Aashuri: Effect of annealing on soft magnetic behavior of nanostructured $(Fe_{0.5}Co_{0.5})_{73.5}Si_{13.5}B_9Nb_3Cu_1$ ribbons. *Alloys Compd.* **582**, 79 (2014).
13. F.G. Chen and Y.G. Wang: Investigation of glass forming ability, thermal stability and soft magnetic properties of melt-spun $Fe_{83}P_{16-x}Si_xCu_1$ (x = 0, 1, 2, 3, 4, 5) alloy ribbons. *Alloys Compd.* **584**, 377 (2014).

14. M. Shi, R. Li, J. Wang, Z. Liu, X. Luo, and T. Zhang: Effects of minor Cu addition on glass-forming ability and magnetic properties of FePCBCu alloys with high saturation magnetization. *Philos. Mag.* **93**(17), 2182 (2013).
15. H.Y. Jung and S. Yi: Enhanced glass forming ability and soft magnetic properties through an optimum Nb addition to a Fe–C–Si–B–P bulk metallic glass. *Intermetallics* **18**, 1936 (2010).
16. H.Y. Jung and S. Yi: Effect of Cu addition on nanocrystallization behaviors and magnetic properties of the $Fe_{76.5-x}C_{6.0}Si_{3.3}B_{5.5}P_{8.7}Cu_x$ (x = 0–3 at.%) bulk metallic glass. *J. Alloys Compd.* **561**, 76 (2013).
17. K. Hono, D.H. Ping, M. Ohnuma, and H. Onodera: Cu clustering and Si partitioning in the early crystallization stage of an $Fe_{73.5}Si_{13.5}B_9Nb_3Cu_1$ amorphous alloy. *Acta Mater.* **47**, 997 (1999).
18. T. Ohkubo, H. Kai, D.H. Ping, K. Hono, and Y. Hirotsu: Mechanism of heterogeneous nucleation of a-Fe nanocrystals from $Fe_{89}Zr_7B_3Cu_1$ amorphous alloy. *Scr. Mater.* **44**, 971 (2001).
19. Y. Yoshizawa and K. Yamauchi: Magnetic-properties of FeCuCrSiB, FeCuVSiB, FeCuMoSiB, alloys. *Mater. Sci. Eng., A* **133**, 176 (1991).
20. W. Lefebvre, S. Morin-Grognet, and F. Danoix: Role of niobium in nanocrystallization of a $Fe_{73.5}Si_{13.5}B_9Nb_3Cu_1$ alloy. *J. Magn. Magn. Mater.* **301**, 343 (2006).
21. S.H. Lim, W.K. Pi, T.H. Noh, H.J. Kim, and I.K. Kang: Effects of Al on the magnetic properties of nanocrystalline $Fe_{73.5}Cu_1Nb_3Si_{13.5}B_9$ alloys. *J. Appl. Phys.* **73**, 6591 (1993).
22. B.J. Tate, B.S. Parmar, I. Todd, H.A. Davies, M.R.J. Gibbs, and R.V. Major: Soft magnetic properties and structures of nanocrystalline Fe-Al-Si-B-Cu-Nb alloy ribbons. *J. Appl. Phys.* **83**, 6335 (1998).
23. J. Moya, M.J. Garcia, M. Vazquez, and H. Sirkin: Role of aluminium in structural and magnetic properties of nanocrystalline alloy FeSiBNbCu. *J. Phys. IV* **8**, 135 (1998).
24. M.W. Chen, A. Sakai, A. Inoue, X.M. Wang, Y. Watanabe, and T. Sakurai: Partitioning behavior of Al in a nanocrystalline FeZrBAl soft magnetic alloy. *J. Appl. Phys.* **87**, 439 (2000).
25. A. Takeuchi and A. Inoue: Classification of bulk metallic glasses by atomic size difference, heat of mixing and period of constituent elements and its application to characterization of the main alloying element. *Mater. Trans.* **46**, 2817 (2005).
26. J.S. Gook, K.K. Lee, D.J. Yoon, and J. Choi: Effect of additional elements (Al, Ga) on the thermal stability of supercooled liquid in Fe-P-C-B-AL-Ga glassy alloys. *J. Kor. Inst. Met. Mater.* **36**, 1757 (1998).
27. N. Chen, L. Martin, D.V. Luzgyune-Luygin, and A. Inoue: Role of alloying additions in glass formation and properties of bulk metallic glasses. *Materials* **3**, 5320 (2010).
28. X.H. Lin and W.L. Johnson: Formation of Ti–Zr–Cu–Ni bulk metallic glasses. *J. Appl. Phys.* **78**, 6514 (1995).
29. B.D. Cullity and C.D. Graham: *Introduction to Magnetic Materials*, 2nd ed. (Wiley-IEEE Press, New Jersey, 2008); 54 pp.
30. M. Ohnuma, K. Hono, S. Linderoth, J.S. Pedersen, Y. Yoshizawa, and H. Onodera: Small-angle neutron scattering and differential scanning calorimetry studies on the copper clustering stage of Fe–Si–B–Nb–Cu nanocrystalline alloys. *Acta Mater.* **48**, 4783 (2000).
31. H.M. Otte: Lattice parameter determinations with an x-ray spectrogoniometer by the Debye-Scherrer method and the effect of specimen condition. *J. Appl. Phys.* **32**, 1536 (1961).
32. H.Y. Jung, M. Stoica, S. Yi, D.H. Kim, and J. Eckert: Crystallization kinetics of $Fe_{76.5-x}C_{6.0}Si_{3.3}B_{5.5}P_{8.7}Cu_x$ (x = 0, 0.5, and 1 at.%) bulk amorphous alloy. *Metall. Mater. Trans. A* (Online) 29 August, 2014, doi: 10.1007/s11661-014-2536-2.